



저작자표시-비영리-변경금지 2.0 대한민국

이용자는 아래의 조건을 따르는 경우에 한하여 자유롭게

- 이 저작물을 복제, 배포, 전송, 전시, 공연 및 방송할 수 있습니다.

다음과 같은 조건을 따라야 합니다:



저작자표시. 귀하는 원저작자를 표시하여야 합니다.



비영리. 귀하는 이 저작물을 영리 목적으로 이용할 수 없습니다.



변경금지. 귀하는 이 저작물을 개작, 변형 또는 가공할 수 없습니다.

- 귀하는, 이 저작물의 재이용이나 배포의 경우, 이 저작물에 적용된 이용허락조건을 명확하게 나타내어야 합니다.
- 저작권자로부터 별도의 허가를 받으면 이러한 조건들은 적용되지 않습니다.

저작권법에 따른 이용자의 권리는 위의 내용에 의하여 영향을 받지 않습니다.

이것은 [이용허락규약\(Legal Code\)](#)을 이해하기 쉽게 요약한 것입니다.

[Disclaimer](#)

Thesis for Master Degree

An Active Heave Compensation System for Offshore Crane
considering the Time-delay

Advisor : Prof. Choi, Hyeong-Sik
Prof. Lee, Moon-Jin



February 2017

Department of Convergence Study on the Ocean Science and
Technology

School of Ocean Science and Technology
Seong, Hyung-Seok

본 논문을 성형석의 공학석사 학위논문으로 인준함.

위원장 김 준 영 (인)

위 원 유 삼 상 (인)

위 원 최 형 석 (인)



2017년 2월

한국해양과학기술원-한국해양대학교

해양과학기술전문대학원

해양과학기술융합학과

본 논문을 성형식의 공학석사 학위논문으로 인준함.

위원장	김 준 영
위 원	유 삼 상
위 원	최 형 식



2017년 2월

한국해양과학기술원-한국해양대학교
해양과학기술전문대학원
해양과학기술융합학과

Table of Contents

Nomenclature	v
List of Tables	vii
List of Figures	viii
Abstract	x

Chapter 1. Introduction	1
1.1 Background and History	1
1.2 Recent research	5
Chapter 2. Mathematical Model of Dynamics	7
2.1 Coordinate of AHC system	7
2.2 Dynamic relations among the forces	10
2.3 Hydraulic-driven winch system dynamics	12
Chapter 3. Control Strategy	14
3.1 PD controller	14
3.2 Sliding mode controller	14
3.3 Nonlinear generalised predictive controller	16

Chapter 4. Simulation and Results	20
4.1 PD controller	22
4.2 Sliding mode controller	24
4.3 Nonlinear generalised predictive controller	28
 Chapter 5. Conclusions	 29
 Appendix	
A.1 Feedback linearization	31
A.2 Predictive control of general nonlinear systems	34
 Acknowledgements	 39
 References	 40



Nomenclature

z	Linear position along the heave direction
l	Rope length
Δl	Rope extension of elastic rope
$\dot{\Delta l}$	Velocity of rope extension
w	Disturbance acting on the crane
l_0	Rope length at initial time
r	Radius of the winch
ψ	Angular displacement of the winch
$\dot{\psi}$	Angular velocity of the winch
c	Elastic coefficient
E	Young's modulus of the rope
A	Intersectional area of the rope
Δl_s	Static rope extension
Δl_d	Dynamic rope extension
F_g	Gravitational force
$F_{cr,s}$	Static spring force of the rope
F_b	Buoyancy force by the hydrostatic lift
m_p	Mass of the payload
$m_{l,r}$	Mass of the rope per length
ρ_w	Density of the water
V	Volume of the payload
l_w	Nominal rope length submerged in water
m_{eq}	Equivalent mass
A_{33}	Added mass coefficient
$F_{cr,d}$	Dynamic spring force
d_r	Damping coefficient of the rope

F_d	Hydrodynamic drag force
C_{ds}	Drag coefficient
A_p	Nominal cross-sectional area for the payload
z_w	Velocity of the ambient water particles
$\ddot{\psi}$	Acceleration of the winch angle
T_w	Time constant of the winch dynamics
$K_{v,w}$	Proportional constant of the flow rate
u_w	Input voltage
i_w	Transmission ratio
$V_{mot,w}$	Volume of the hydraulic motor



List of Tables

Table 4.1 Parameters used for the simulation in analyzing numerically 4



List of Figures

Fig. 1.1 The offshore crane in operation	1
Fig. 1.2 The offshore crane in harsh condition	2
Fig. 1.3 The suspended payload	3
Fig. 1.4 Motion reference unit	5
Fig. 2.1 The whole sketch of AHC system	8
Fig. 2.2 Dominant movement in AHC system	8
Fig. 2.3 Without heave compensation ; general explanation	9
Fig. 2.4 AHC winch and the payload	9
Fig. 2.5 Actual picture of AHC winch	13
Fig. 4.1 Outer loop for simulation	21
Fig. 4.2 Inner loop for simulation	21
Fig. 4.3 The block diagram for active heaving compensation system	22
Fig. 4.4 Dynamic response for $w(t) = 0.5 \sin 5t$	23
Fig. 4.5 Dynamic response for $w(t) = 0.8 \sin 0.5t - 0.8 \sin(0.5t - 0.9)$	23
Fig. 4.6 Dynamic response with PD control for $w(t) = 0.5 \sin 5t$	24
Fig. 4.7 Dynamic response with SMC for $w(t) = 0.5 \sin 5t$	25
Fig. 4.8 Dynamic response with SMC for $w(t) = 0.8 \sin 0.5t - 0.8 \sin(0.5t - 0.9)$	26
Fig. 4.9 The time-delay factors on active heaving compensation system	27
Fig. 4.10 Dynamic response with 1s time-delay and SMC for $w(t) = 0.5 \sin 5t$	27
Fig. 4.11 Dynamic response with 1s time-delay also SMC and NGPC for $w(t) = 0.5 \sin 5t$	28

시간 지연을 고려한 해상 크레인의 상하동요 보상 시스템의 능동제어

Seong, Hyung Seok

Department of Convergence Study on the Ocean Science and Technology

Ocean Science and Technology School
Korea Maritime and Ocean University

Abstract

This thesis presents a heave compensation system for offshore crane when it gets unexpected disturbances and external force. The dynamic model consists of crane assumed to be the rigid body, hydraulic driven winch, elastic rope and payload. To keep the payload from moving up and down, PD control is applied by using linearization. For better performance, sliding mode control and nonlinear generalized predictive control algorithm is applied due to the time-delay. As a result, the oscillating amplitude of the payload is reduced by using the control algorithm. Considering the time-delay assumed one second involved in the system, nonlinear generalized predictive controller with robust controller is suitable control algorithm for this heave compensation system because it makes the position of payload reach the desired position with least error. In the end of thesis, it shows the control algorithm using the robust control and its simulation results.

KEY WORDS: Active heave compensation 상하동요 능동제어; Nonlinear system 비선형 시스템; Sliding mode control 슬라이딩 모드 제어; Time-delay 시간 지연; Nonlinear generalized predictive control 비선형 일반 예측 제어.

Chapter 1. Introduction

1.1 Background and History

With the demand for offshore platform in the deep sea, the installation depth of offshore platforms has been deeper and the size of them has been larger. Also the maintenance and repair for the installed platform including the subsea exploration around them have extended the range from the sea along the coast to the sea far from the coast whose depth is over 3000 m. Moreover, these tasks are needed in the difficult situation such as in the Arctic Ocean. So the position control of the offshore crane which is operated for working in those kinds of situation has become important. When the offshore crane is working on the sea with the environmental loading such as ocean waves, tidal currents, or winds such as shown in Fig. 1.1. the position control of the offshore crane does matter. Since they cause the crane (or vessel) to place away from the desired position both horizontally and vertically. There have been lots of heated discussions, a number of control techniques and studies for dealing with the position control for horizontal motion. However, the position control for vertical motion has not attracted researcher's attention.



Fig. 1.1 The offshore crane in operation



Fig. 1.2 The offshore crane in harsh condition

To ensure the functionality of the crane system under harsh sea conditions such as the situation described in Fig. 1.2, it is important to prevent the payload motion from moving unaffected by the environmental loading-induced crane motion. So the object is to safe and accurate positioning operate when transferring, or holding the payload shown in Fig. 1.3. It is crucial to consider the tension of the rope which the payload is attached to because it causes the damping dynamics in underwater condition. In addition, the unwanted vertical motion of the payload should be reduced noticeably regardless of the environmental loading.

The problem of safe and accurate position control for the offshore crane in tough sea conditions has been addressed by many publications in the past. Especially, in the view of vertical position control, there are two types of control for heave compensation. The first one is called passive heave compensation (PHC). PHC is a technique used to reduce the effect of waves or other unwanted disturbance upon lifting and drilling operations. A simple passive heave compensator is a soft spring which acts like a vibration isolator. The main principle in PHC is to store the energy from the external forces influencing the system where the input

is ship motion and output is a reduced amplitude motion of attached one. Therefore, shock absorbers or drilling compensators are simple forms of PHC.



Fig. 1.3 The suspended payload

Another approach is to use the active heave compensator which applies a force onto the load. This system is called active heave compensation (AHC) system. AHC is a technique used on lifting equipment to reduce the influence of waves or other environmental loading upon offshore operations. There are difference between PHC and AHC system in that AHC system is an actual control system actively trying to compensating for any movement at a desired position. A control system is often based on programmable logic controller and it calculates how the active parts of the system should react to the movement. Therefore, the performance of an AHC system is limited by motor speed, torque, energy or power, by measurement accuracy and its delay, or by computing algorithms. It does matter to choose the control method that which kind of control algorithm used to preset values or delayed signals, considering other environmental loading.

Among the first active heave systems Southerland (1970) showed the mechanical handling systems which evaluates the ship motion and payload response to various sea conditions. The

control method of relative motion compensation and load attenuation was studied where the system is a spring-loaded tether. By pulling in and out the tether, a hydraulic proportional valve was adjusted to keep the payload constant height from the deck.

The mechanically actuated system was presented by Blanchet and Reynolds (1977) and patented. A heave compensator package capable of transferring heavy loads was invented to compensate an accurate fine positioning control of the load.

In 1980s, Barber (1982) invented a control system for a motion compensating arrangement which stabilizes a body suspended by a flexible line from a support structure. This system was circuit based AHC system so that it was capable of detecting and sensing the heave motion. From this invention, the study for a support structure subject to uncontrolled or unwanted disturbance causing oscillating movements began.

In the meantime, the theory and algorithm of AHC system were developed in the sonar field. Hutchins (1978) invented a heave compensation system for an underwater towed seismic system. The system has a circuit having simple double integrator converting accelerometer data into vertical motion data. A pressure transducer located in a support structure produced a pressure signal indicative of the depth so that the sonar array used for mapping the ocean bottom by using the circuit. By measuring the vertical position data, the system made the sonar array adjust the sonar pulse timing, correcting for vertical motion.

This kind of method using the sonar data to correct the vertical motion, improved method was invented by El-Hawary (1982). By applying fast fourier transform (FFT) to measured sonar data, the frequency components of heave motion were analyzed. Then by means of Kalman filter, it was able to establish a refined value of the high frequency important in getting an accurate account of the seabed profile.

As late as 1990s, Jones and Cherbonnier (1990) invented the motion compensation system especially, concerning multiple actuators and control mechanisms. Integrating typically existing compensators and their circuits, this control system advantageously included an hydraulic fluid pump, and a four-way directional control valve to use multiple actuators. This kind of

practical and specializing in heave compensating system was presented by Robichaux and Hatleskog (1993). The system using microprocessor and a responsive operator was particularly useful in improving the operational results of hydraulic or pneumatic drill string compensators on floating drilling rigs. The system was based on a microprocessor control including mechanical hardware and software adjusting the control parameters to multiple platforms such as marine vessels, floating offshore drilling rigs or traveling blocks. This improved system made operator modify only software part by changing several parameters which cost less expensive than before also it broadened the AHC system application field.

It does matter to diminish vessel heave motion from the drill strings when the drilling vessels is drilling at sea. That purpose was in accord with the one of AHC system so that research had been conducted by applying AHC system to the drilling system. Korde (1988) removed the effect on the drill-ships from heave motion which it made the operating time longer and them stable. In this system, the simulation showed complete decoupled dynamic system by using the linear model which utilized the accelerometer data for position and force feedback. After then, the research for nonlinear model based control system has been suggested for application by Do and Pan (2008).

1.1.2 Recent research

To acquire the heave motion of the offshore crane effected by disturbance on the sea in the real time, the modern system uses an inertial measurement unit(IMU) such as shown in Fig. 1.4.



Fig. 1.4 Motion reference unit

By Using 3-axis accelerometers and gyroscopes, an IMU determines ship motion. Since the payload is attached to the end of the rope, between sensors and control systems there are time delays in the input-output signal system. It is critical to design the control system with the time delay minimized. Kyllingstad (2012) came up with the transfer function filter to adjust the phase or time lag for minimizing time delay. On the other hand, Kuchler, et al., (2011) used heave prediction algorithms to estimate and predict the heave motion of the vessel based on previous measurements and then applied control action based on these predicted motions.



Chapter 2. Mathematical Model of Dynamics

In order to formulate control system for any dynamic model, it is important to understand background knowledge and fundamental concepts about the processes and physical laws governing the dynamics. With respect to AHC system, factors for instance dynamic forces acting on the offshore crane, hydraulic-driven winch system, elastic forces due to rope and various forces on the payload should be considered. This chapter introduces some of these fundamental ideas and concepts about AHC system with describing above factors minutely.

2.1 Coordinate of AHC system

AHC system consists of the offshore crane, the hydraulic-driven winch and the payload cling to the elastic rope. The offshore crane is considered as a rigid body system for simplicity. The hydraulic-driven winch system is acting like a first-order dynamic system. Since AHC system concentrates upon estimating and compensating the heave motion of the payload, only the vertical motion coordinate is defined. That makes horizontal forces acting on the system neglected, so are any random currents. Furthermore, the offshore crane is not affected by the motion of payload because it is considered as rigid body. The control purpose of AHC system is to maintain the position of the payload when it is located at the deep sea.

The system coordinate has 1-DOF; only z axis is considered. As to understand the whole pictures, Fig. 2.1 depicts the overall dynamic factors. And only the z axis position is considered here, Fig. 2.2 and Fig. 2.3 help to understand the whole concept. The z axis represents the position of payload which points along depth length under the sea. Note that the z axis is zero at the surface and points downwards; hence, it is positive for increasing depth.

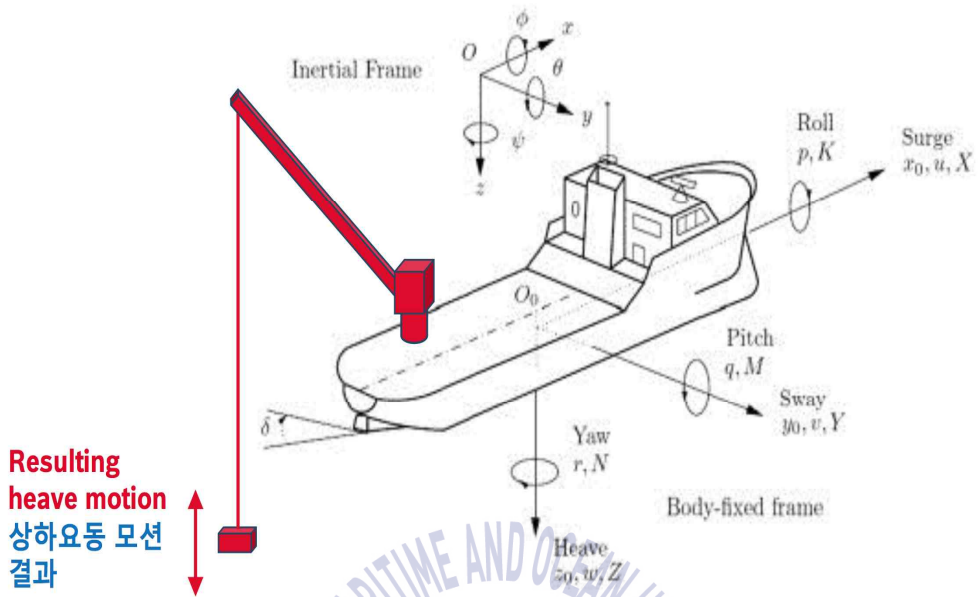


Fig. 2.1 The whole sketch of AHC system

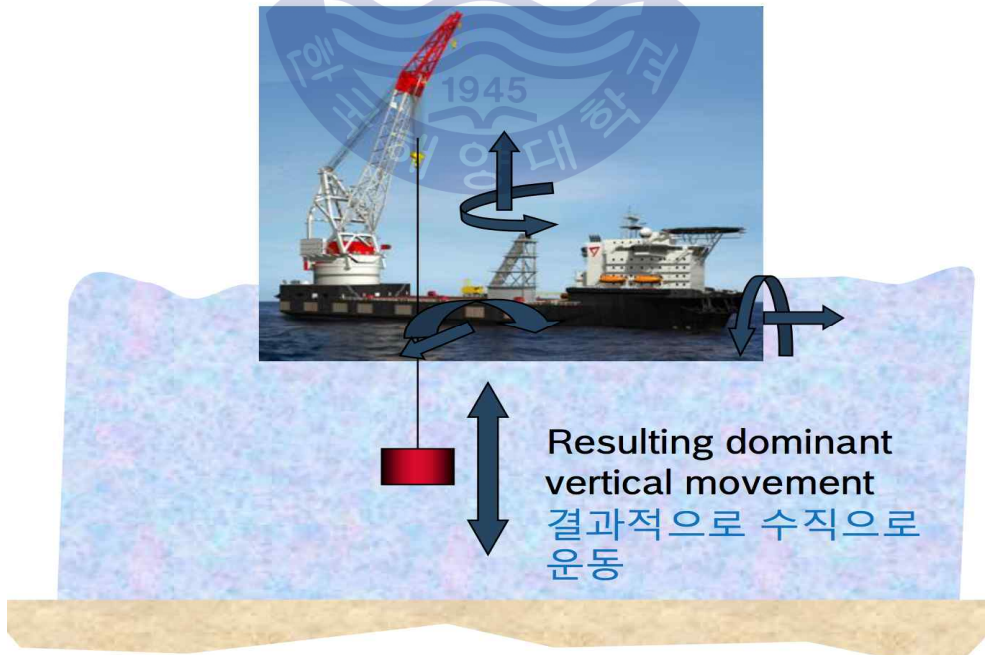


Fig. 2.2 Dominant movement in AHC system

General explanation

Without heave compensation

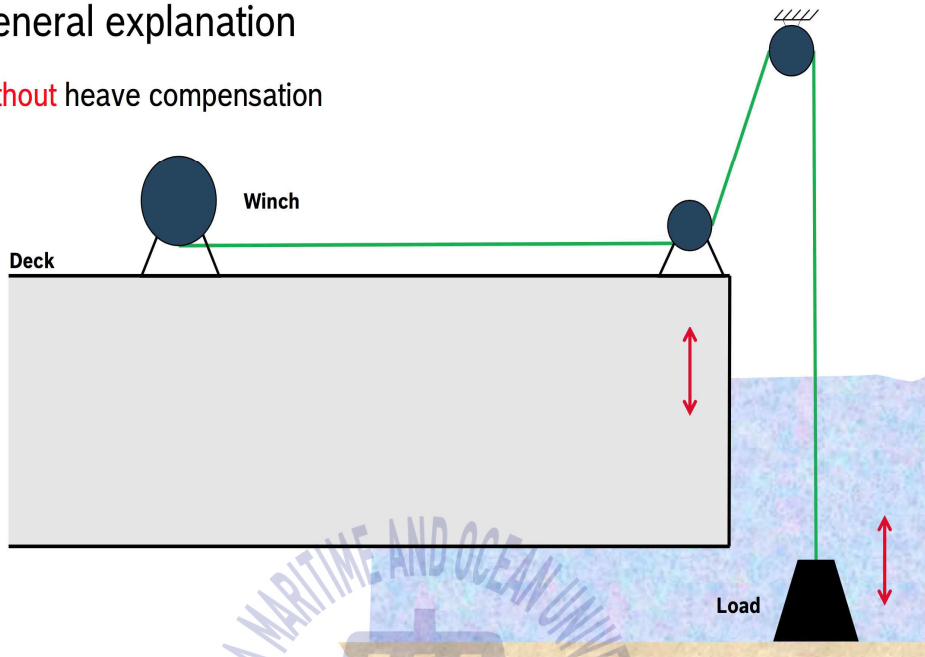


Fig. 2.3 Without heave compensation ; general explanation

The position of the payload $z(t)$ consists of the length of rope l , the extension of elastic rope Δl and payload motion effected by the offshore crane disturbances acting on w . So the position of the payload $z(t)$ is defined by equation (2.1).

$$z(t) = l(t) + \Delta l(t) + w(t) \quad (2.1)$$

For the winch system, the hydraulic-driven winch is located at the top of offshore crane. Because only 1 degree is considered and above assumption changes the offset of the origin of the rope so that it does not break any characteristics of dynamic model. The length of rope depends upon the angle of winch and is defined as equation (2.2)

$$l(t) = l_0 + r\psi(t) \quad (2.2)$$

where l_0 denotes the rope length at initial time, r denotes the radius of the winch and $\psi(t)$ denotes the angular displacement of the winch.

The rope is elastic so that it has elastic coefficient defined by (2.3).

$$c = E \frac{A}{l} \quad (2.3)$$

Here E is the Young's modulus of the rope and A denotes the intersectional area of the rope.

Since the elastic rope oscillates under the sea, the extension of rope length is divided into a static part and a dynamic part as in (2.4)

$$\Delta l(t) = \Delta l_s + \Delta l_d \quad (2.4)$$

where Δl_s and Δl_d denote the static rope extension and the dynamic rope extension, respectively.

2.2 Dynamic relations among the forces

From the rope extension, the forces acting on AHC system are described in this section. The static rope extension is given by the static equilibrium of forces which is written as following equation (2.5)

$$F_g = F_{cr,s} + F_b \quad (2.5)$$

where F_g denotes the gravitational force, $F_{cr,s}$ denotes the static spring force of the rope and F_b denotes the buoyancy force caused by the hydrostatic lift. The gravitational force F_g is given by equation (2.6)

$$F_g = g (m_p + \frac{1}{2} m_{l,r} l) \quad (2.6)$$

where g denotes the gravitational constant, m_p denotes the mass of payload and $m_{l,r}$ denotes the mass of the rope per meter. The static spring force of the rope $F_{cr,s}$ is given by equation (2.7).

$$F_{cr,s} = \frac{EA}{l} \Delta l_s \quad (2.7)$$

And the buoyancy force F_b is given by equation (2.8)

$$F_b = \rho_w g \left(V + \frac{1}{2} A l_w \right) \quad (2.8)$$

where ρ_w denotes the density of the water, V denotes the volume of the payload and l_w denotes the nominal rope length submerged in water.

The equivalent mass for AHC system is given by equation (2.9)

$$m_{eq} = m_p + A_{33} + \frac{1}{3} m_{l,r} l \quad (2.9)$$

where A_{33} denotes the added mass coefficient term accounting for the heave motion of the payload submerged in water.

The dynamic rope extension caused by the motion of offshore crane and payload can be obtained by applying to Newton's second formula. Equation (2.10) shows the dynamic relations

$$m_{eq} \ddot{z} = -F_{cr,d} - F_{dr} - F_d \quad (2.10)$$

where \ddot{z} denotes the acceleration of the payload, $F_{cr,d}$ denotes the dynamic spring force, F_{dr} denotes the rope's damping force and F_d denotes the hydrodynamic drag force. The dynamic spring force $F_{cr,d}$ is given by equation (2.11)

$$F_{cr,d} = \frac{EA}{l} \Delta l_d \quad (2.11)$$

The damping force of the rope is given by equation (2.12)

$$F_{dr} = d_r \Delta \dot{l}_d \quad (2.12)$$

where d_r denotes the damping coefficient of the rope. The hydrodynamic drag force F_d is given by equation (2.13)

$$F_d = \frac{1}{2} \rho_w C_{ds} A_p (\dot{z} - \dot{z}_w) |\dot{z} - \dot{z}_w| \quad (2.13)$$

where C_{ds} denotes the drag coefficient, A_p denotes the payload's nominal cross-sectional area in the heave direction and \dot{z}_w denotes the velocity of the ambient water particles which

is neglected because it is assumed that the payload is submerged far below the water surface.

2.3 Hydraulic-driven winch system dynamics

In the AHC system, the control input is given by the hydraulic-driven winch system. The dynamic equation of hydraulic-driven winch system is given by equation (2.14)

$$\ddot{\psi} = -\frac{1}{T_w} \dot{\psi} + \frac{2\pi K_{v,w}}{i_w V_{mot,w} T_w} u_w \quad (2.14)$$

where $\ddot{\psi}$ denotes the acceleration of the winch angle, $\dot{\psi}$ denotes the velocity of the winch angle, T_w denotes the time constant of the winch dynamics, $K_{v,w}$ denotes the proportional constant of the flow rate to the input voltage u_w , i_w denotes the transmission ratio and $V_{mot,w}$ denotes the volume of the hydraulic motor. Here the sketch of AHC winch is drawn in Fig. 2.4 also the actual AHC winch is shown in Fig. 2.5.

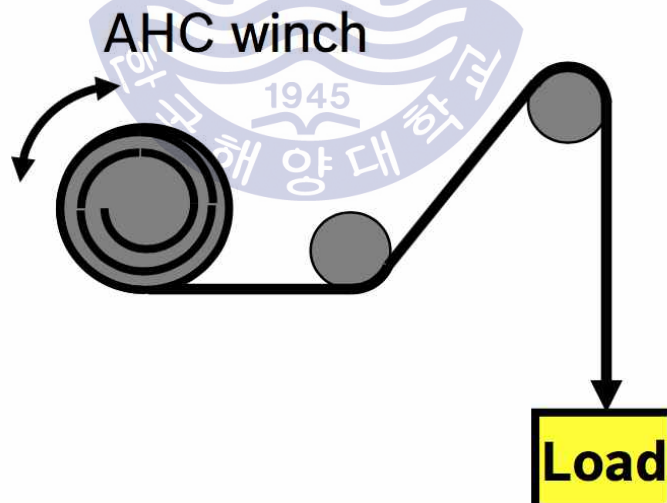


Fig. 2.4 Sketch of AHC winch and the payload



Fig. 2.5 Actual picture of AHC winch



Chapter 3. Control strategy

3.1 PD Controller

In AHC system, the position of the payload is measured in real time by using the inertial measurement unit(IMU). The control purpose is to keep the position of the payload still so the error is defined as the difference between the desired trajectory and its actual position. From the above definition, PD(Proportional-Derivative) controller is applied to AHC system in order that the motion of the payload is reduced. Since the hydraulic-driven winch dynamics is simple differential equation with the second order, the solution which shows the relation equation between the rotational angle and control input is easily acquired as shown in equation (3.1).

$$\psi(t) = (1 - e^{-T/t_w}) \frac{2\pi K_{v,w}}{i_w V_{mot,w}} u_w(t) \quad (3.1)$$

By using the linearization for the input-output relation equations, the output is written as in equation (3.2)

$$z(t) = l(0) + w(t) - \frac{ml(0)}{EA} [\Delta \dot{i}(t) + \ddot{w}(t)] + [1 + \frac{m}{EA} (\Delta \dot{i}(t) + \ddot{w}(t))] r \psi(t) \quad (3.2)$$

from the equation (3.2), the PD control input is attained.

3.2 Sliding mode controller

From the chapter 2, the dynamic equations can be transformed into the state-space equation as following equation (3.3)

$$\mathbf{x} = [x_1 \ x_2 \ x_3 \ x_4]^T = [\Delta l_{r,d} \ \Delta \dot{l}_{r,d} \ \psi_w \ \dot{\psi}_w]^T \quad (3.3)$$

In this notation, the dynamic equations can be written in equation (3.4)

$$\dot{\mathbf{x}} = f(\mathbf{x}) + g u(t) + d(t), \quad \mathbf{y} = C \mathbf{x}, \quad t \geq 0 \quad (3.4)$$

$$f(\mathbf{x}) = \begin{bmatrix} x_2 \\ -\frac{EA}{m_{eq}(l_0 + r x_3)} + \frac{r}{T_w} x_4 \\ x_4 \\ -\frac{1}{T_w} x_4 \end{bmatrix}$$

$$g = \left[0 \quad -\frac{2\pi r K_{v,w}}{i_w V_{mot,w} T_w} \quad 0 \quad -\frac{2\pi K_{v,w}}{i_w V_{mot,w} T_w} \right]^T$$

where $f(x)$ denotes the dynamic characteristics of the system, g denotes the constant matrix for control input which indicates the characteristics of the winch system, $d(t)$ denotes the disturbance included in the system and C denotes the matrix for adjusting the constant parameters for the output.

The robust controller is quite suitable choice where uncertain disturbances and parameters exist because it effectively cancels out them. Especially, in that AHC system has nonlinear characteristics and uncertain parameters also unwanted disturbances, sliding mode controller(SMC) is a reasonable choice to handle this system. SMC is the robust controller for the disturbance also the uncertain parameters while this controller is easily applied to the nonlinear system, too (Young, et al.,1999). As mentioned above, the error is defined as the error which is the difference between the desired trajectory and current position. In addition, another error is defined as the difference between the desired velocity and current velocity. These definitions make the sliding surface s by using the errors as in equation (3.5)

$$s = \mathbf{y} - \mathbf{y}_d + \lambda (\dot{\mathbf{y}} - \dot{\mathbf{y}}_d) \quad (3.5)$$

The sliding surface is convergent to zero where Lyapunov stability is satisfied which means that the purpose of control is achieved in AHC system. The error which denotes the difference between the desired trajectory and current position as \tilde{y} , and error which denotes the difference between the desired velocity and current velocity as $\dot{\tilde{y}}$ makes equation (3.5) as following equations (3.6) and (3.7)

$$\dot{s} = 0 = \dot{\mathbf{y}} - \dot{\mathbf{y}}_d + \lambda \ddot{\mathbf{y}} \quad (3.6)$$

$$\dot{\mathbf{y}} = \dot{\mathbf{y}}_d - \lambda \ddot{\mathbf{y}} \quad (3.7)$$

From the above equations (3.4) and (3.7), the relation equation of errors is attained as equation (3.8)

$$Cf(\mathbf{x}) + Cg u - \dot{\mathbf{y}}_d + \lambda \ddot{\mathbf{y}} = 0 \quad (3.8)$$

In order to satisfy the sliding surface equation $\dot{s} = 0$, the equivalent control input \hat{u} is calculated as in equation (3.9)

$$\hat{u} = [Cg]^{-1} [\dot{\mathbf{y}}_d - \lambda \ddot{\mathbf{y}} - Cf(\mathbf{x})] \quad (3.9)$$

So the control input for SMC is as following in equation (3.10)

$$u = \hat{u} + \Delta u = \hat{u} - k(\mathbf{x}, t) \text{sgn}(s(t)) \quad (3.10)$$

where the parametric conditions for $k(\mathbf{x}, t)$ is as in equation (3.11)

$$k(\mathbf{x}, t) = F(\mathbf{x}, t) + \eta, \quad \eta > 0 \quad (3.11)$$

The above equation (3.11) shows the sliding condition for satisfying the Lyapunov stability. The constrained condition for parameters including uncertainties are as following equations (3.12), (3.13).

$$|\hat{f}(\mathbf{x}, t) - f(\mathbf{x}, t)| \leq F(\mathbf{x}, t) \quad (3.12)$$

$$\frac{1}{2} \frac{d}{dt} s^2 = s \dot{s} = [Cf(\mathbf{x}) - C\hat{f}(\mathbf{x})] s(t) - k(\mathbf{x}, t) |s(t)| \leq \eta |s(t)| \quad (3.13)$$

3.3 Nonlinear generalized predictive controller

In the circumstances where the disturbances and unexpected or uncertain parameters exist, to control the nonlinear system, the nonlinear generalised predictive control (NGPC) is one of the most promising algorithms (Chen, et al., 2003). For applying the nonlinear system, the extended results from the appendix A.2 are used in this section.

The following assumptions are imposed on the nonlinear system given by equation (3.4) :

(A1) The zero dynamics are stable.

(A2) All states are available.

(A3) Each of the system output $y(t)$ has the same well-defined relative degree ρ .

(A4) The output $y(t)$ and the reference signal $r(t)$ are sufficiently many times continuously differentiable with respect to t .

The output prediction procedures are given by the Taylor series expansion. In the moving time frame, repeated differentiation up to ρ times of the output \hat{y} with regard to time is needed. Since the relative degree is one here, equation (3.14) denotes the repeated substitution of AHC system where the output Cx is assumed to be $h(x)$ for the conventional notation.

$$\hat{y}(t) = L_f h(x) = \frac{\partial h(x)}{\partial x} f(x) = x_2 + r_w x_4 \quad (3.14)$$

For deriving the control input from the nonlinear system, one more differentiation is needed shown in equation (3.15).

$$\hat{y}(t)^{[\rho+1]} = L_f^{\rho+1} h(x) + p_{11}(\hat{u}(t), x(t)) + L_g L_f^{\rho-1} h(x) \hat{u}(t) \quad (3.15)$$

where p_{11} denotes the equation (3.16)

$$p_{11}(\hat{u}(t), x(t)) = L_g L_f^{\rho} h(x) \hat{u}(t) + \frac{d L_g L_f^{\rho-1} h(x)}{dt} \hat{u}(t) \quad (3.16)$$

From the equation (3.15), $\hat{y}(t)^{[2]}$ is calculated as shown in equation (3.17)

$$\begin{aligned} \hat{y}(t)^{[2]} &= L_f^2 h(x) + p_{11}(\hat{u}(t), x(t)) + L_g h(x) \hat{u}(t) \\ &= -\frac{E_r A_r x_1}{m_{eq}[l(0) + r_w x_3]} + L_g L_f h(x) \hat{u}(t) + L_g h(x) \hat{u}(t) \end{aligned} \quad (3.17)$$

The output predicted matrix is given by the equation (3.18)

$$\widehat{Y}(t) = \begin{bmatrix} \widehat{y}(t)^{[0]} \\ \widehat{y}(t)^{[1]} \\ \widehat{y}(t)^{[2]} \end{bmatrix} = \begin{bmatrix} h(x) \\ L_f^1 h(x) \\ L_f^2 h(x) \end{bmatrix} + \begin{bmatrix} 0 \\ 0 \\ H(\widehat{u}) \end{bmatrix} \quad (3.18)$$

where $H(\widehat{u})$ denotes a matrix valued function of control inputs as shown in the equation (3.19)

$$H(\widehat{u}) = [p_{11}(\widehat{u}(t), x(t)) + L_g h(x) \widehat{u}(t)] \quad (3.19)$$

From the equations (3.15) to (3.19), the output $\widehat{y}(t+\tau)$ at time τ is practically predicted by the equation (3.20)

$$\widehat{y}(t+\tau) \simeq T(\tau) \widehat{Y}(t) = [I \ \bar{\tau}] \widehat{Y}(t) \quad (3.20)$$

Here the matrix $T(\tau)$ and $\bar{\tau}$ given by shown in the equation (3.21) and (3.22)

$$T(\tau) = [I \ \bar{\tau}] \quad (3.21)$$

$$\bar{\tau} = \left[1 \ \tau \ \frac{\tau^2}{2!} \right] \quad (3.22)$$

Also to get the $\widehat{r}(t+\tau)$ at time τ is given by the Taylor expansion of $r(t)$. This reference signal is given by the equation (3.23)

$$\widehat{r}(t+\tau) = T(\tau) \widehat{R}(t) = T(\tau) [r(t)^T \ \dot{r}(t)^T] \quad (3.23)$$

Considering the time delay, this is given by the Taylor series expansion by using the following matrix \bar{T} as shown in the equation (3.24)

$$\bar{T}_{(i,j)} = \frac{\bar{N}^{i+j+1}}{(i-1)!(j-1)!(i+j-1)} \quad (3.24)$$

where \bar{N}^{i+j-1} denotes moving horizon time frame interval matrix. The following equation (3.25) denotes the control input for the system.

$$u = - (L_g L_f^{\rho-1} h(x))^{-1} (KM_{\rho} + L_f^{\rho} h(x) - w^{\rho}(t)) \quad (3.25)$$

where ρ denotes the relative degree for the system and $w(t)$ denotes the desired trajectory function. The matrix K and M denotes the attained tracking trajectory and the

predictive trajectory calculated by the Taylor expansion. The matrix M is given by the equation (3.26).

$$M_{(\rho=1)} = \begin{pmatrix} h(x) - w(t) \\ L_f^1 h(x) - w^{[1]}(t) \end{pmatrix} \quad (3.26)$$



Chapter 4. Simulation Results

In this chapter, a series of control algorithm on the AHC system is utilized. At first, in the view of practical application where actual operating offshore crane is being utilized the specification and parameters for simulation of AHC system are shown as in Table 4.1.

Table 4.1 Parameters used for the simulation in analyzing numerically

Symbol	Description	Units	Value
E	Young's modulus	N/m^2	200×10^9
A	Intersection of the cable	m^2	$\pi \times (0.025)^2$
l_0	Length of the cable	m	2000
m_{eq}	Equivalent mass	kg	3.8×10^3
T_w	Time constant	-	0.07
r_w	Radius of the winch	m	1

Simulation time is 100 second and the unwanted disturbances are assumed to be the regular wave source $w(t) = 0.5 \sin 5t$ and $w(t) = 0.8 \sin 0.5t - 0.8 \sin(0.5t - 0.9)$. In this thesis, the simulation tool is Simulink. Whole simulation consists of two parts which are inner loop and outer loop for simulation. Fig. 4.1 shows outer loop for simulation and Fig. 4.2 shows inner loop which consists of all the dynamics and control algorithms, respectively. As described above, the position of the payload is measured in real time by using the inertial measurement unit(IMU) and the two errors which are position error between the desired position and actual position and velocity error between the desired velocity and actual velocity are utilized for the control algorithm.

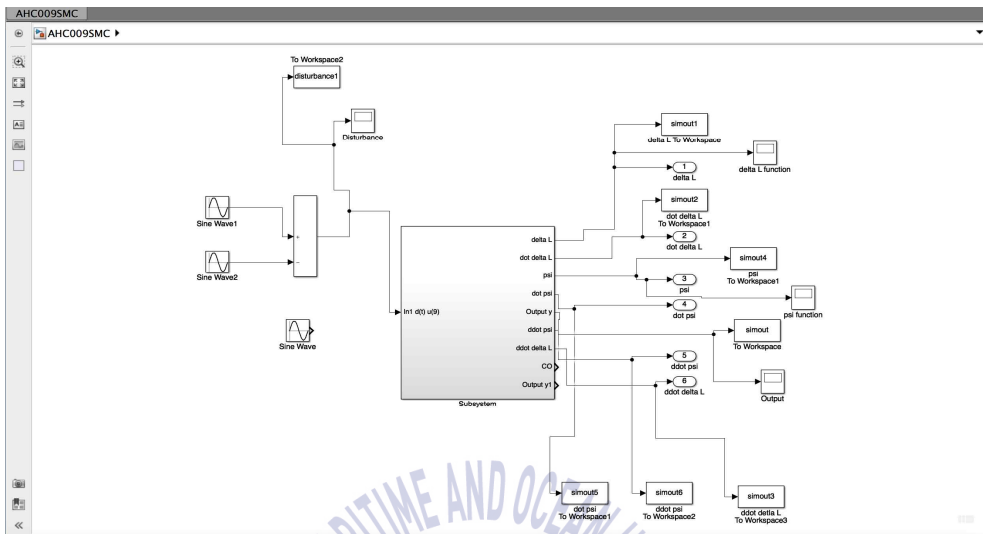


Fig. 4.1 Outer loop for simulation

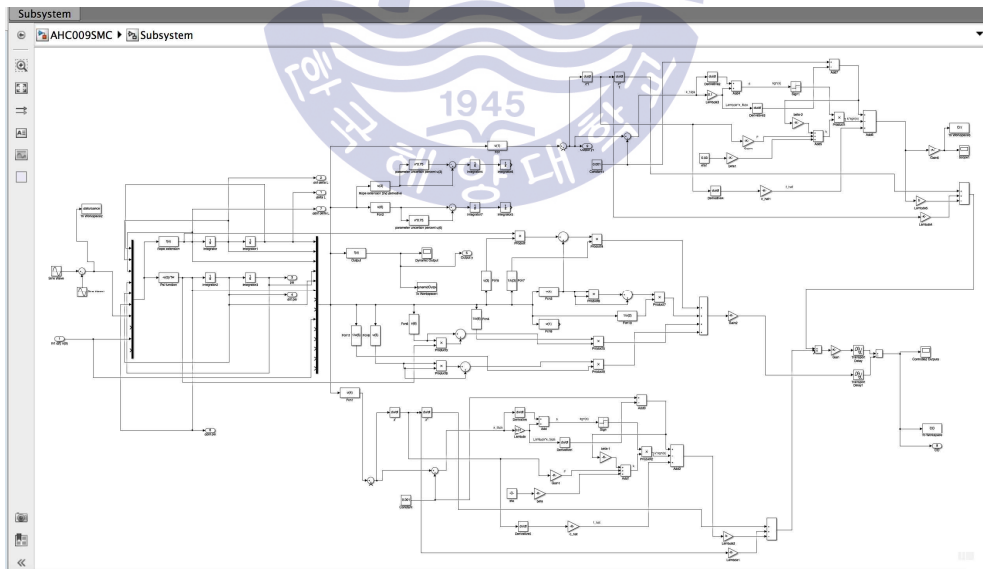


Fig. 4.2 Inner loop for simulation

4.1 PD Controller

The entire block diagram for AHC system is shown in Fig.4.3. As the entire system consists of dynamic system, disturbance, controller, winch encoder, and sensor, Fig.4.3 shows the whole flow of the AHC system. PD control algorithm is input to the system as a controller in the block diagram.

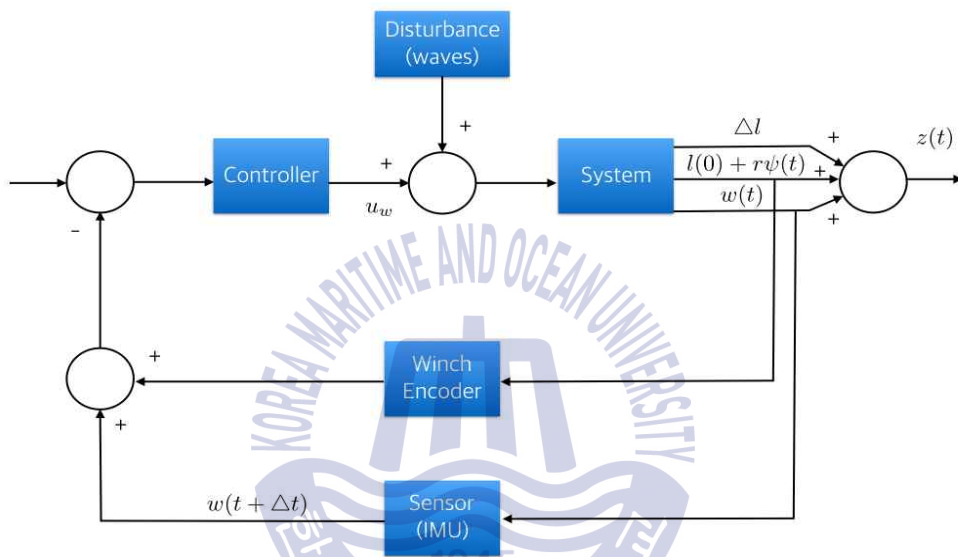


Fig. 4.3 The block diagram for active heaving compensation system

At first, the characteristic of the dynamic of AHC system is shown in Fig. 4.4 and Fig. 4.5. As shown in Fig. 4.4 and Fig. 4.5, the dynamic characteristic of AHC system is oscillating movement of payload. Due to the disturbance assumed to be the regular wave while on the sea actual disturbance is the irregular wave which however, is not considered in this study, the motion of the payload is oscillating, obviously. Its maximum displacement is 0.58m where the origin of the payload is located at 2,000m under the sea.

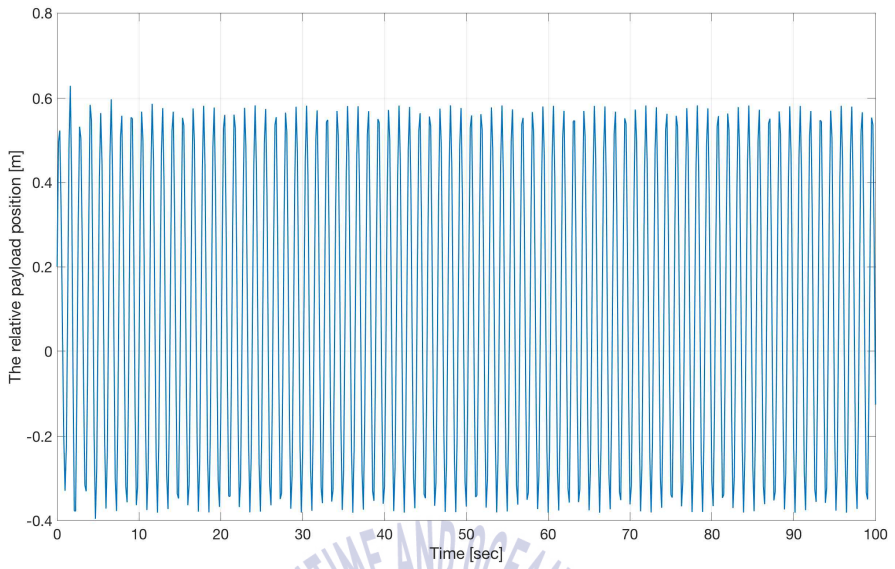


Fig. 4.4 Dynamic response for $w(t) = 0.5 \sin 5t$

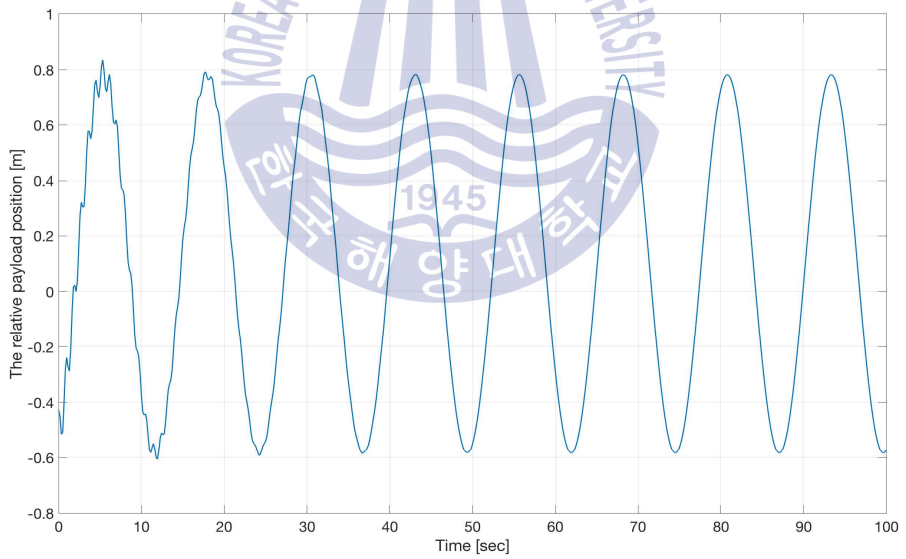


Fig. 4.5 Dynamic response for $w(t) = 0.8 \sin 0.5t - 0.8 \sin(0.5t - 0.9)$

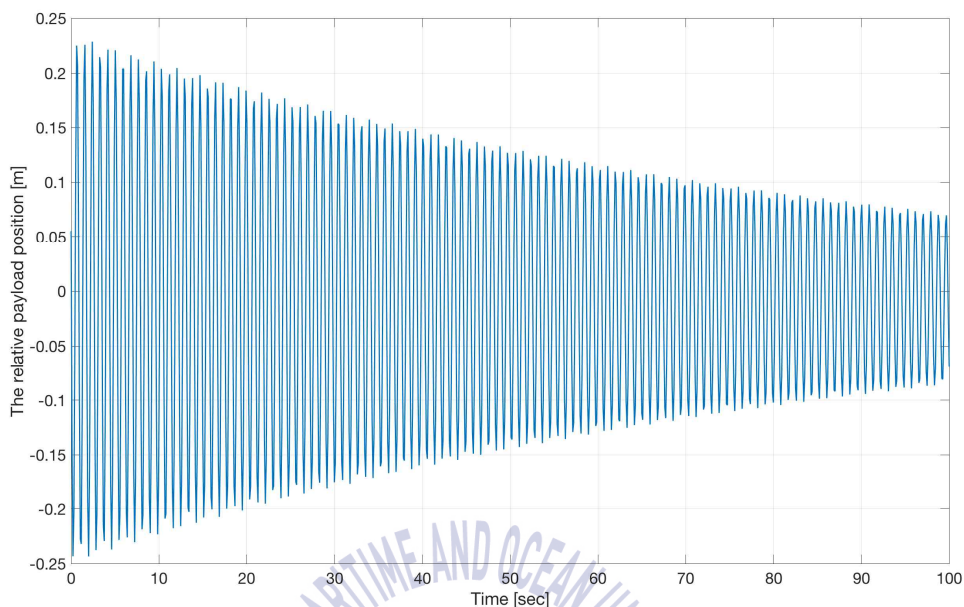


Fig. 4.6 Dynamic response with PD control for $w(t) = 0.5 \sin 5t$

As shown in Fig. 4.6, when PD control is applied, the relative motion of payload is decreased into 0.082m. The effect of the PD control is clearly seen since the displacement of payload is decreased as expected. After comparing with the graphs in Fig. 4.4 to 4.6, they show the similar tendency that the movement of payload is oscillating. Since the PD control is originally reducing the amplitude of its variables, it looks like PD control algorithm is well applied to this system.

4.2 Sliding mode controller

Since the sliding mode controller(SMC) is robust controller for the rigid body system and the offshore crane is assumed to be rigid body, it looks plausible to apply SMC to AHC system. Also the SMC is based on the error dynamics, the sliding surface is defined as error multiplied by gain constant given by sliding surface condition and Lyapunov stability. In this study, only the numerical analysis is conducted, however, the uncertain parameters and gains are calculated properly to decrease the motion of payload. The relative motion of the payload

with SMC algorithm applied is shown in Fig. 4.7.

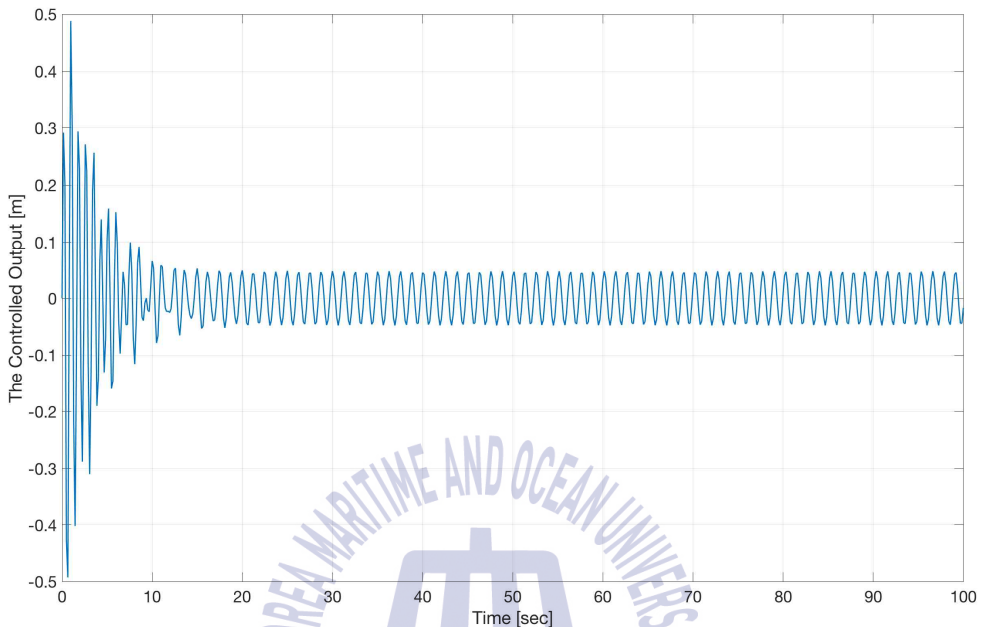


Fig. 4.7 Dynamic response with SMC for $w(t) = 0.5 \sin 5t$

As comparing the Fig. 4.4 to 4.7, the result graph with SMC applied clearly shows the effect of robust control. The maximum amplitude of the payload is reduced into 0.0602m. While the chattering exists, the amplitude is only in about 10% compared to the original dynamic characteristic already has. Since the SMC has chattering, also the dynamic characteristic is oscillating. It doesn't matter what kind of controller is used to this system, because the oscillating motion is not removed.

Also as comparing the Fig. 4.5 to Fig. 4.8, Fig. 4.8 shows the effect of SMC. The low frequency disturbance makes the controlled output stable at the end while the chattering is a little bit remained.

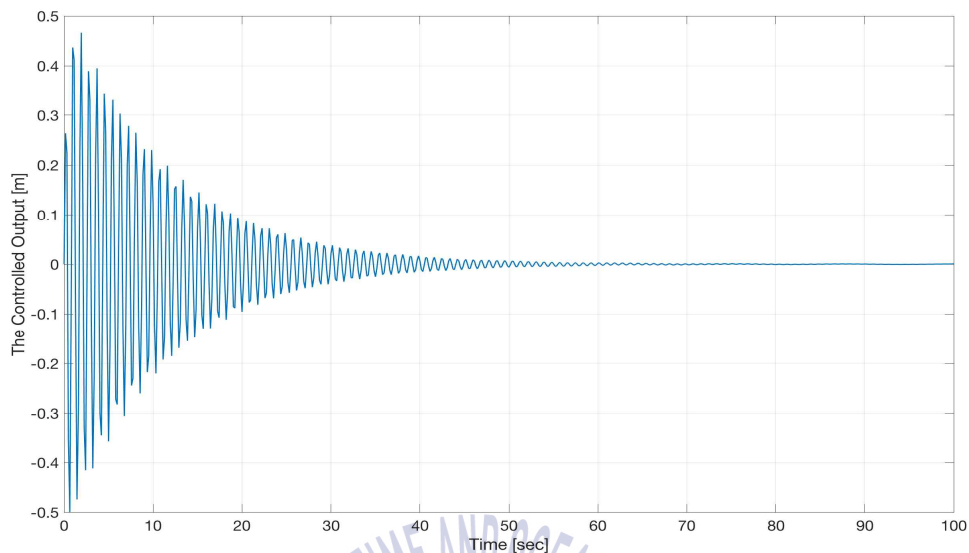


Fig. 4.8 Dynamic response with SMC for $w(t) = 0.8 \sin 0.5t - 0.8 \sin(0.5t - 0.9)$

As AHC system has time-delay problem. It's obvious seen from the Fig. 4.9 which shows the whole block diagram relating with the SMC applied. Since the dynamics parameters and variables are detected by the sensors, got calculated by winch encoder, and are to be used to derive the control algorithms, there are time-delay between the sensors and other devices. Actually, time-delay is the main issues to signal-system part but in this paper, only the 1 second time-delay existing is considered for the simulation.

So if the 1 second time-delay is considered for above controller, Fig. 4.10 shows the retarded graph tendency compared to Fig. 4.7.

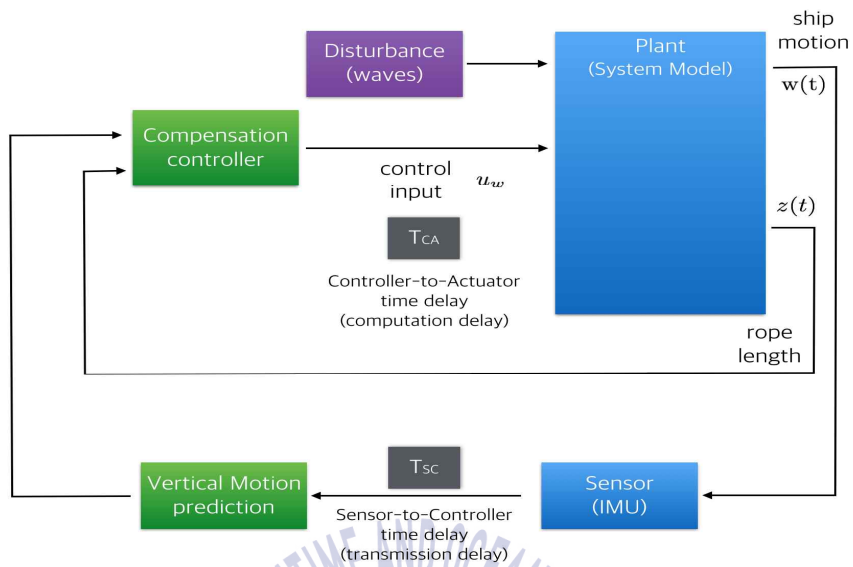


Fig 4.9 The time-delay factors on active heaving compensation system

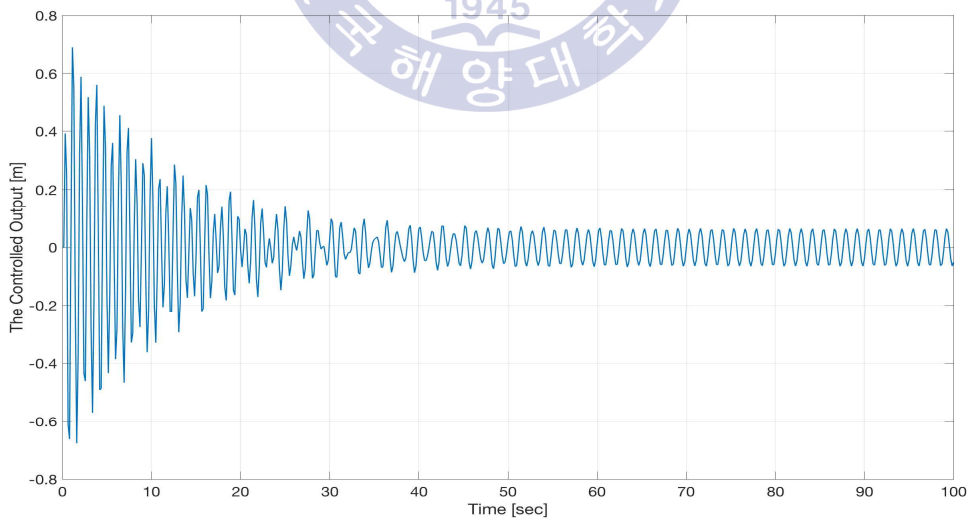


Fig 4.10 Dynamic response with 1s time-delay and SMC for $w(t) = 0.5 \sin 5t$

4.3 Nonlinear generalised predictive controller

Assumed SMC algorithm already applied, nonlinear generalised predictive controller (NGPC) can dwindle the first period of oscillation amplitude due to the predictive algorithm. Also, once in a stable stage, the amplitude(the relative motion of the payload) is a little reduced due to NGPC. It means that SMC is a robust controller so that the other controller combined in the same system can not affect much.

In this section, the simulation result which the combined controller including both SMC and NGPC shows is shown in Fig. 4.11.

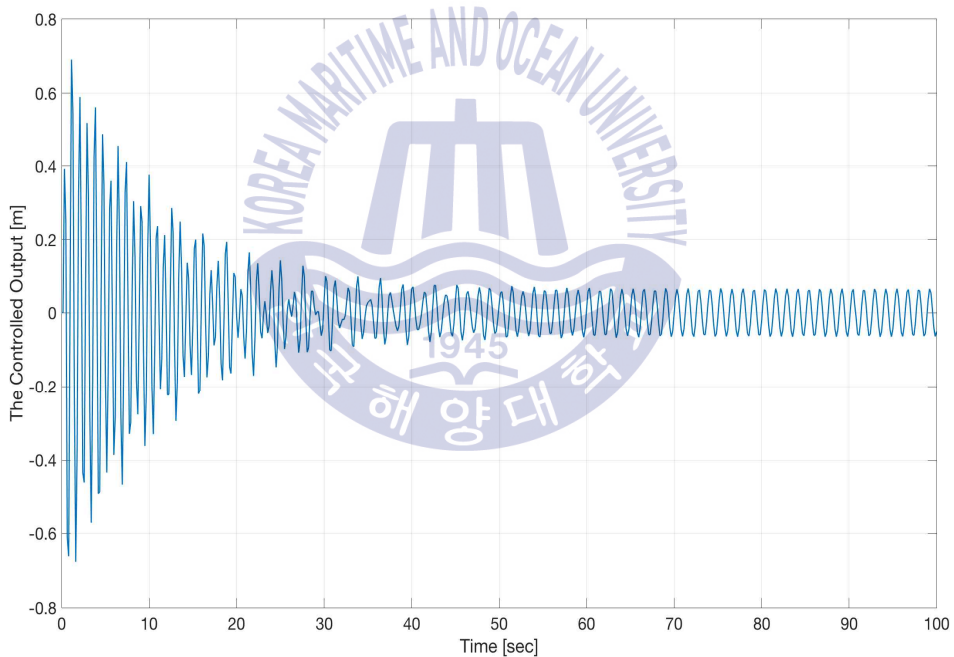


Figure 4.11 Dynamic response with 1s time-delay also SMC and NGPC for $w(t) = 0.5 \sin 5t$

Since the SMC and NGPC are both applied, the maximum amplitude of oscillating payload is reduced into 0.0524m. And as already mentioned above, the first period of oscillating amplitude is a little decreased.

Chapter 5. Conclusions

In this thesis, heave compensation control system which consists of the offshore crane assumed to be the rigid body, the hydraulic-driven winch, the elastic rope and the payload is modeled by mathematically and implemented in a simulation. The purpose of control is to maintain the relative motion of the payload from the reference point in still and the important variable in this system is the dynamic variation of the elastic rope's length. That's why to control the relative motion of the payload, dynamic model is set including the dynamic variation of the elastic rope's length and the rotational angular variable of winch.

As for controlling the position of the payload, PD control algorithm is the first option to choose. Since the purpose of the control is matched, and the characteristics of error dynamic are shown in AHC system. By using PD controller, the simulation shows the maximum amplitude is reduced into 0.13m from 0.58m where no controller is used.

In the view of the error dynamics, the robust controller, i.e., here the sliding mode controller is proposed and used for simulation. Since SMC does effectively cancel out the disturbance and handle with other unexpected or uncertain parameters, actually the simulation result shows the dramatically reduced amplitude change about 90%. Also the time-delay is a issue on this system because the payload is located at under the deep sea, the detected information and calculating time should be considered. So the time-delay is assumed to be 1 second and due to nonlinear characteristic of this system, nonlinear generalised predictive control algorithm is used for dealing with the time-delay. NGPC doesn't affect much the amplitude since combined robust controller, here, SMC. The simulation result which is using both SMC and NGPC shows only the a little reduced amplitude change from the former simulations. Obviously, SMC is effectively canceling out the disturbances and leaving the chattering on the system, no other controller combined with SMC would show the effective amplitude change in the system. However, in this thesis, only the regular wave acts a disturbance source which could be the reason for above result. So in the case the irregular wave sources or similar wave forms are input to the system, NGPC could do more than.

Also the time-delay is in this thesis 1 second assumed, more precise and practical calculated time-delay is needed for further research.



Appendix A

A.1 Feedback linearization

Another way to get feedback linearization of nonlinear system is to construct a nonlinear control law as a so-called inner loop control (Spong, et al., 2004). It means that by a suitable state space change of coordination, the nonlinear system is changed into the feedback linearizable system. The new coordinates of the transformed system satisfy with the traditional control deesign specifications for instance tracking and disturbance rejection.

From the equation (3.4), the whole AHC system is transformed into equation (A.1) by the suitable change of coordinate.

$$y = T(x), \dot{y} = Ay + Bv = \frac{\partial T}{\partial x} \dot{x} \quad (\text{A.1})$$

where $T(x)$ denotes the nonlinear change of coordinate. In this system, the control input is given by the equation (A.2).

$$u = \frac{1}{\langle dT_n, g \rangle} (v - \langle dT_n, f \rangle) \quad (\text{A.2})$$

In advance, to use the above control law, conditions for Frobenius theorem should be verified. The following equations (A.3) ~ (A.8) are needed to verify.

$$g = [0 \quad -br_w \quad 0 \quad b]^T \quad (\text{A.3})$$

where b denotes $\frac{2\pi K_{v,w}}{i_w V_{mot,w} T_w}$ for simplification.

$$ad_f(g) = [br_w - \frac{br_w}{T_w} \quad -b \quad \frac{b}{T_w}]^T \quad (\text{A.4})$$

here the $ad_f^k(g)$ denotes $[f, ad_f^{k-1}(g)]$, also $[f, g]$ is the Lie bracket of f and g , which makes a third vector field defined by $[f, g] = \frac{\partial g}{\partial x} f - \frac{\partial f}{\partial x} g$.

$$ad_f^2(g) = \left[\frac{br_w}{T} - \frac{A_r E_r br_w}{m_{eq}(l_0 + r_w x_3)} - \frac{br_w}{T_w^2} + \frac{A_r E_r br_w}{[m_{eq}(l_0 + r_w x_3)]^2} x_1 - \frac{b}{T_w} - \frac{b}{T_w^2} \right]^T \quad (A.5)$$

$$ad_f^3(g) = \left[a_1 \quad a_2 \quad -\frac{b}{T_w} \quad \frac{b}{T_w^3} \right]^T \quad (A.6)$$

where a_1 and a_2 are respectively,

$$a_1 = \frac{br_w}{T_w^2} - \frac{A_r E_r br_w}{m_{eq}(l_0 + r_w x_3)} - \frac{A_r E_r br_w x_1}{m_{eq}l_0^2 + 2T_w m_{eq}l_0 r_w x_e + m_{eq}r_w^2 x_3^2} \quad (A.7)$$

$$a_2 = \frac{A_r E_r br_w}{T_w m_{eq}(l_0 + r_w x_3)} - \frac{br_w}{T_w^3} + \frac{A_r E_r br_w x_1}{T_w m_{eq}l_0^2 + 2T_w m_{eq}l_0 r_w x_3 + T_w m_{eq}r_w^2 x_3^2} \quad (A.8)$$

$$+ \frac{A_r E_r br_w x_2}{m_{eq}l_0^2 + 2m_{eq}l_0 r_w x_3 + m_{eq}r_w^2 x_3^2} - \frac{A_r E_r br_w^2 x_4}{m_{eq}l_0^2 + 2m_{eq}l_0 r_w x_3 + m_{eq}r_w^2 x_3^2}$$

$$- \frac{2A_r E_r br_w^2 x_1 x_4}{m_{eq}l_0^3 + 3m_{eq}l_0 r_w x_3 + 3m_{eq}l_0 r_w^2 x_3^2 + m_{eq}r_w^3 x_3^3}$$

Since the rank of $[g \quad ad_f(g) \quad ad_f^2(g) \quad ad_f^3(g)]$ is 4, the conditions are satisfied with so that the new coordinate can be assigned into $y_i = T_i$. Take the simplest solution shown in equation (A.9), other coordinates are attained consequently which are shown in equations (A.10), (A.11) and (A.12)

$$y_1 = T_1 = x_1 \quad (A.9)$$

$$y_2 = T_2 = \langle dT_1, f \rangle = \sum_{i=1}^4 \frac{\partial T_1}{\partial x_i} f_i = x_2 \quad (A.10)$$

$$y_3 = T_3 = \langle dT_2, f \rangle = \sum_{i=1}^4 \frac{\partial T_2}{\partial x_i} f_i = -\frac{E_r A_r}{m_{eq}(l_0 + r_w x_3)} x_1 + \frac{r_w}{T_w} x_4 \quad (A.11)$$

$$y_4 = T_4 = \langle dT_3, f \rangle = \sum_{i=1}^4 \frac{\partial T_3}{\partial x_i} f_i = \quad (A.12)$$

$$- \frac{E_r A_r}{m_{eq}(l_0 + r_w x_3)} x_2 + \frac{E_r A_r m_{eq} r_w x_1 x_4}{[m_{eq}(l_0 + r_w x_3)]^2} - \frac{r_w}{T_w^2} x_4$$

The control law here is equation (A.2), so equation (A.13) is needed to get $\langle dT_4, g \rangle$

$$\langle dT_4, g \rangle = \sum_{i=1}^4 \frac{\partial T_4}{\partial x_i} g_i = \frac{E_r A_r b r_w}{m_{eq} (l_0 + r_w x_3)} + \frac{m_{eq} r_w E_r A_r x_1}{[m_{eq} (l_0 + r_w x_3)]^2} - \frac{r_w b}{T_w} \quad (\text{A.13})$$

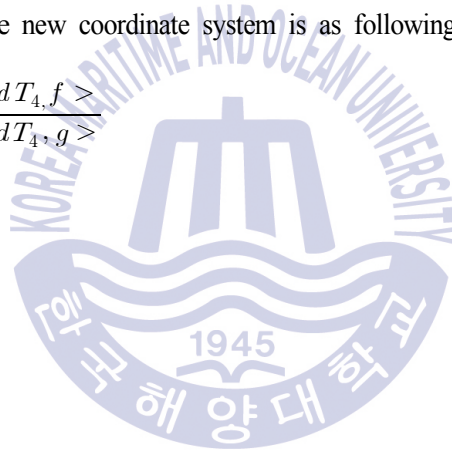
also the equation (A.14) is needed to get $\langle dT_4, f \rangle$

$$\begin{aligned} \langle dT_4, f \rangle &= \sum_{i=1}^4 \frac{\partial T_4}{\partial x_i} f_i \\ &= \frac{C_2}{C_1} \left\{ 2m_{eq} r_w x_2 x_4 + C_2 x_1 - C_1 \frac{r_w x_4}{T_w} + 2 \frac{C_2 m_{eq}^2 r_w^2}{C_1} x_1 x_4^2 - x_4 x_1 \frac{m_{eq} r_w}{T_w} \right\} \\ &+ x_4 \frac{r_w}{T_w^3} \end{aligned} \quad (\text{A.14})$$

where $C_1 = C_1(x_3) = m_{eq} (l_0 + r_w x_3)$, $C_2 = E_r A_r$ for simplification, respectively.

The control input for the new coordinate system is as following equation (A.15).

$$u = \frac{v}{\langle dT_4, g \rangle} - \frac{\langle dT_4, f \rangle}{\langle dT_4, g \rangle} \quad (\text{A.15})$$



A.2 Predictive control of general nonlinear systems

An single-input-single-output(SISO) general nonlinear system can be described by the equation (A.16)

$$\begin{cases} \dot{\mathbf{x}}(t) = \mathbf{f}(\mathbf{x}(t), u(t)) \\ y(t) = h(\mathbf{x}(t)) \end{cases} \quad (\text{A.16})$$

where $x \in R^n$, $u \in R$ and $y \in R$ are state, input and output respectively. The results developed in this section are capable of extending to multivariable general nonlinear systems.

For the sake of simplicity, the following notation is introduced in this section :

$$D_{\mathbf{f}} h(\mathbf{x}) = \frac{\partial h(\mathbf{x})}{\partial \mathbf{x}} \mathbf{f}(\mathbf{x}, u) \quad (\text{A.17})$$

$$D_{\mathbf{f}_z}^k h(\mathbf{x}) = \frac{\partial D_{\mathbf{f}_z}^{k-1} h(\mathbf{x})}{\partial \mathbf{x}} \mathbf{f}(\mathbf{x}, u) \quad \text{for } k > 1 \quad (\text{A.18})$$

$$D_u D_{\mathbf{f}_z}^k h(\mathbf{x}) = \frac{\partial D_{\mathbf{f}_z}^k h(\mathbf{x})}{\partial u} \quad (\text{A.19})$$

Suppose that the output of the nonlinear system in the prediction horizon is approximated by its Taylor series expansion up to order $r \geq \mu$. One has

$$y(t + \tau) \approx y(t) + \tau \dot{y}(t) + \dots + \frac{\tau^r}{r!} y^{[r]}(t), \quad T_1 \leq \tau \leq T_2 \quad (\text{A.20})$$

The derivatives of the output required in the approximation are given by

$$\dot{y}(t) = \frac{\partial h(\mathbf{x})}{\partial \mathbf{x}} \dot{\mathbf{x}} = \frac{\partial h(\mathbf{x})}{\partial \mathbf{x}} \mathbf{f}(\mathbf{x}, u) = D_{\mathbf{f}_z} h(\mathbf{x}) \quad (\text{A.21})$$

and

$$\ddot{y}(t) = \frac{\partial}{\partial \mathbf{x}} \left(\frac{\partial h(\mathbf{x})}{\partial \mathbf{x}} \mathbf{f}(\mathbf{x}, u) \right) \dot{\mathbf{x}} + \frac{\partial}{\partial u} \left(\frac{\partial h(\mathbf{x})}{\partial \mathbf{x}} \mathbf{f}(\mathbf{x}, u) \right) \dot{u} = D_{\mathbf{f}_x}^2 h(\mathbf{x}) \quad (\text{A.22})$$

The last equality follows from the notation in (A.17), (A.18). Similarly, one has

$$y^{[k]}(t) = D_{\mathbf{f}_x}^k h(\mathbf{x}), \text{ for } k = 3, \dots, \mu \quad (\text{A.23})$$

and

$$y^{[\mu+1]}(t) = \frac{\partial D_{\mathbf{f}_x}^\mu}{\partial \mathbf{x}} \mathbf{f}(\mathbf{x}, u) + \frac{\partial D_{\mathbf{f}_x}^\mu}{\partial u} \dot{u} = D_{\mathbf{f}_x}^{\mu+1} h(\mathbf{x}) + D_u D_{\mathbf{f}_x}^\mu h(\mathbf{x}) \dot{u} \quad (\text{A.24})$$

Differentiation of $y^{[\mu+1]}$ with respect to time t and substitution of the system's dynamics gives

$$\begin{aligned} y^{[\mu+2]} &= \frac{\partial D_{\mathbf{f}_x}^{\mu+1} h(\mathbf{x})}{\partial \mathbf{x}} \mathbf{f}(\mathbf{x}, u) + \frac{\partial D_{\mathbf{f}_x}^{\mu+1} h(\mathbf{x})}{\partial u} \dot{u} + \frac{\partial D_u D_{\mathbf{f}_x}^\mu h(\mathbf{x})}{\partial \mathbf{x}} \mathbf{f}(\mathbf{x}, u) \dot{u} \\ &\quad + \frac{\partial D_u D_{\mathbf{f}_x}^\mu h(\mathbf{x})}{\partial u} \dot{u}^2 + D_u D_{\mathbf{f}_x}^\mu h(\mathbf{x}) \ddot{u} \\ &= D_{\mathbf{f}_x}^{\mu+2} h(\mathbf{x}) + D_u D_{\mathbf{f}_x}^\mu h(\mathbf{x}) \ddot{u} + z_1(\mathbf{x}, u, \dot{u}) \end{aligned} \quad (\text{A.25})$$

where

$$z_1(\mathbf{x}, u, \dot{u}) = \frac{\partial D_{\mathbf{f}_x}^{\mu+1} h(\mathbf{x})}{\partial u} \dot{u} + \frac{\partial D_u D_{\mathbf{f}_x}^\mu h(\mathbf{x})}{\partial \mathbf{x}} \mathbf{f}(\mathbf{x}, u) \dot{u} + \frac{\partial D_u D_{\mathbf{f}_x}^\mu h(\mathbf{x})}{\partial u} \dot{u}^2 \quad (\text{A.26})$$

Repeating the above procedure, the higher order derivatives can be calculated until the r th order derivative, which given by

$$y^{[r]}(t) = D_{\mathbf{f}_x}^r h(\mathbf{x}) + D_u D_{\mathbf{f}_x}^\mu h(\mathbf{x}) u^{[r-\mu]} + z_{r-\mu-1}(\mathbf{x}, u, \dot{u}, \dots, u^{[r-\mu-1]}) \quad (\text{A.27})$$

where $z_{r-\mu-1}(\mathbf{x}, u, \dot{u}, \dots, u^{[r-\mu-1]})$ is a complicated nonlinear function of $\mathbf{x}, u, \dot{u}, \dots, u^{[r-\mu-1]}$.

Invoking (A.27) into (A.20), the output in the receding horizon is approximated by its Taylor expansion to the order r as

$$y(t+\tau) \approx \tau \mathbf{Y}, \quad T_1 \leq \tau \leq T_2 \quad (\text{A.28})$$

where

$$\boldsymbol{\tau} = [1 \quad \tau \quad \cdots \quad \frac{\tau^r}{r!}] \quad (\text{A.29})$$

and

$$\mathbf{Y}(t) = [y^{[0]}(t) \quad y^{[1]}(t) \quad \cdots \quad y^{[\mu]}(t) \quad y^{[\mu+1]}(t) \quad y^{[\mu+2]}(t) \quad \cdots \quad y^{[r]}(t)]^T \quad (\text{A.30})$$

$$= \begin{bmatrix} h(\mathbf{x}) \\ D_{\mathbf{f}_x} h(\mathbf{x}) \\ \vdots \\ D_{\mathbf{f}_x}^\mu h(\mathbf{x}) \\ D_{\mathbf{f}_x}^{\mu+1} h(\mathbf{x}) \\ D_{\mathbf{f}_x}^{\mu+2} h(\mathbf{x}) \\ \vdots \\ D_{\mathbf{f}_x}^r h(\mathbf{x}) \end{bmatrix} + \begin{bmatrix} 0 \\ 0 \\ \vdots \\ 0 \\ D_u D_{\mathbf{f}_x}^\mu h(\mathbf{x}) \dot{u} \\ D_u D_{\mathbf{f}_x}^\mu h(\mathbf{x}) \dot{u} + z_1(\mathbf{x}, u, \dot{u}) \\ \vdots \\ D_u D_{\mathbf{f}_x}^\mu h(\mathbf{x}) u^{[r-\mu]} + z_{r-\mu-1}(\mathbf{x}, u, \dot{u}, \dots, u^{[r-\mu-1]}) \end{bmatrix}$$

In the same fashion, the command $w(t+\tau)$ in the receding horizon can be also be approximated by its Taylor series expansion to order r as

$$w(t+\tau) = \boldsymbol{\tau} \mathbf{w} \quad (\text{A.31})$$

where

$$\mathbf{w}(t) = [w^{[0]}(t) \quad w^{[1]}(t) \quad \cdots \quad w^{[\mu]}(t) \quad w^{[\mu+1]}(t) \quad \cdots \quad w^{[r]}(t)]^T \quad (\text{A.32})$$

After approximating the output of the nonlinear system (A.1) and the reference to be tracked by series expansion, the tracking error then can be calculated by

$$e(t+\tau) = y(t+\tau) - w(t+\tau) \approx \boldsymbol{\tau} (\mathbf{Y}(t) - \mathbf{w}(t)) \quad (\text{A.33})$$

Thus the predictive control performance can be approximated by

$$\begin{aligned} J &\approx \frac{1}{2} \int_{T_1}^{T_2} (\mathbf{Y}(t) - \mathbf{w}(t))^T \boldsymbol{\tau}^T \boldsymbol{\tau} (\mathbf{Y}(t) - \mathbf{w}(t)) dt \\ &= \frac{1}{2} (\mathbf{Y}(t) - \mathbf{w}(t))^T \int_{T_1}^{T_2} \boldsymbol{\tau}^T \tau dt (\mathbf{Y}(t) - \mathbf{w}(t)) \\ &= \frac{1}{2} (\mathbf{Y}(t) - \mathbf{w}(t))^T \mathbf{T} (\mathbf{Y}(t) - \mathbf{w}(t)) \end{aligned} \quad (\text{A.34})$$

where

$$\mathbf{T} = \int_{T_1}^{T_2} \boldsymbol{\tau}^T \boldsymbol{\tau} d\tau \quad (\text{A.35})$$

$$= \begin{bmatrix} T_2 - T_1 & \frac{T_2^2 - T_1^2}{2} & \dots & \frac{T_2^{r+1} - T_1^{r+1}}{(r+1)!} \\ \frac{T_2^2 - T_1^2}{2} & \frac{T_2^3 - T_1^3}{3} & \dots & \frac{T_2^{r+2} - T_1^{r+2}}{r!(r+2)} \\ \frac{T_2^{r+1} - T_1^{r+1}}{(r+1)!} & \frac{T_2^{r+2} - T_1^{r+2}}{r!(r+2)} & \dots & \frac{T_2^{2r+1} - T_1^{2r+1}}{r!(2r+1)} \end{bmatrix}$$

At the time t , MPC attempts to find the optimal control profile in the receding horizon, $u(t+\tau), 0 \leq \tau \leq T_2$, to minimise the tracking error. After the nonlinear system (A.16) is approximated by its Taylor series expansion up to the order r , the highest derivative of the control required is $r - \mu$. Hence all the control profile in the receding horizon can be parametrized by

$$u(t+\tau) = u(t) + \tau \dot{u}(t) + \dots + \frac{\tau^{r-\mu}}{(r-\mu)!} u^{[r-\mu]}(t) \quad (\text{A.36})$$

Therefore, instead of minimising the performance index J in terms of the control profile $u(t+\tau), 0 \leq \tau \leq T_2$ directly, the performance index J can be minimised in terms of variables $u(t), \dot{u}(t), \dots, u^{[r-\mu]}(t)$. However, for a general nonlinear under consideration as in (A.1), the control u does not appear in a linear manner and it is difficult to give the explicit solution for u . To avoid this problem, the control u is considered as a new state variable, and the performance J is minimised in terms of $\dot{u}(t), \dots, u^{[r-\mu]}(t)$.

The necessary condition for the optimality is given by

$$\frac{\partial J}{\partial \mathbf{u}} = 0 \quad (\text{A.37})$$

where

$$\mathbf{u} = [\dot{u}(t), \dots, u^{[r-\mu]}(t)]^T \quad (\text{A.38})$$

When the tracking error is approximated by its Taylor series expansion up to order $r \geq \mu$,

the NMPC is given by

$$u(t) = \int \dot{u}(\sigma) d\sigma \quad (\text{A.39})$$

where

$$\dot{u}(\sigma) = -(D_u D_{f_z}^\mu h(\mathbf{x}))^{-1} (\mathbf{K} M_\mu(\sigma) + D_{f_z}^{\mu+1} h(\mathbf{x}) - w^{[\mu+1]}(\sigma)) \quad (\text{A.40})$$

$$M_\mu(\sigma) = \begin{bmatrix} h(\mathbf{x}) - w(\sigma) \\ D_{f_z}^1 h(\mathbf{x}) - w^{[1]}(\sigma) \\ \dots \\ D_{f_z}^\mu h(\mathbf{x}) - w^{[\mu]}(\sigma) \end{bmatrix} \quad (\text{A.41})$$

and $\mathbf{K} \in R^{\mu+1}$ is the first row of the matrix $\mathbf{T}_{rr} \mathbf{T}_{\mu r}^T$,

$$\mathbf{T}_{\mu r} = \begin{bmatrix} \frac{T_2^{\mu+2} - T_1^{\mu+2}}{(\mu+1)!(\mu+2)} & \dots & \frac{T_2^{2\mu+2} - T_1^{2\mu+2}}{\mu!(\mu+1)!(2\mu+2)} \\ \vdots & \vdots & \vdots \\ \frac{T_2^{r+1} - T_1^{r+1}}{(r+1)!} & \dots & \frac{T_2^{r+\mu+1} - T_1^{r+\mu-1}}{\mu! r! (r+\mu+1)} \end{bmatrix}, \quad (\text{A.42})$$

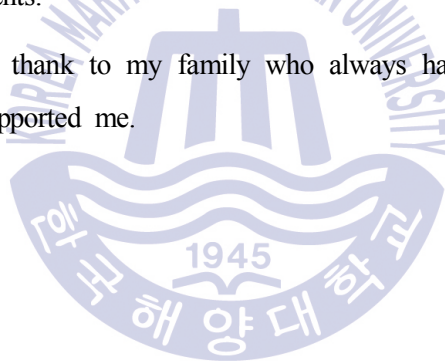
$$\mathbf{T}_{rr} = \begin{bmatrix} \frac{T_2^{2\mu+3} - T_1^{2\mu+3}}{(\mu+1)!(\mu+1)!(2\mu+3)} & \dots & \frac{T_2^{r+\mu+2} - T_1^{r+\mu+2}}{(\mu+1)! r! (r+\mu+2)} \\ \vdots & \vdots & \vdots \\ \frac{T_2^{r+\mu+2} - T_1^{r+\mu+2}}{(\mu+1)! r! (r+\mu+2)} & \dots & \frac{T_2^{2r+1} - T_1^{2r+1}}{r! r! (2r+1)} \end{bmatrix} \quad (\text{A.43})$$

Acknowledgements

I would like to express my sincere gratitude to Prof. Hyeong Sik Choi, Department of Convergence Study on the Ocean Science and Technology Korea Maritime and Ocean University, Korea for his priceless advice and continuous encouragement for my study. I also thank to my committee members, Prof. Jun Young Kim and Sam Sang Yoo for their critical advices for my thesis.

For my senior and juniors in the laboratory, Mr. Jin Il Kang, Sang Gi Jeong, Ji Yoon Oh, Dae Hyung Ji, Seong Won Cho, Dong Wook Jeong, Mai The Vu and Nguyen Ngoc Duc. I warmly thank for their help at all the things where we have been through both good and bad moments.

Finally, I would like to thank to my family who always have faith on me also have loved, encouraged and supported me.



References

- Barber, N.R., GEC Mechanical Handling Limited., 1982. *Control means for motion compensation devices*. US Patent No. 4349179.
- Blanchet, J.P., and Reynolds, T.J., Western Gear Corporation., 1977. *Crane hook heave compensator and method of transferring loads*. US Patent No. 4003472.
- Chen, W.H., Ballance, D.J. and Gawthrop, P.J., 2003. Optimal control of nonlinear system: a predictive control approach. *Automatica*, 39(4), pp.631-644.
- Do, K.D., and Pan, J., 2008. Nonlinear control of an active heave compensation system. *Ocean Engineering*, 35(5-6), pp.558-571.
- El-Hawary, F., 1982. Compensation for source heave by use of a Kalman filter. *IEEE Journal of Ocean Engineering*, 7(2), pp.89-96.
- Hutchins, R., Hunter (70) Limited., 1978. *Heave compensation system*. US Patent 4091356.
- Jones, A.B., and Cherbonnier, T.D., A.R.M. Design Development. 1990. *Active reference System*. US Patent 4962817.
- Kuchler, S., Mahl, T., Neupert, J., Schneider, K. and Sawodny, O., 2011. Active control for an offshore crane using prediction of the vessels motion. *IEEE/ASME Transactions on Mechatronics*, 16(2), pp.297-309.
- Kyllingstad, A., Varco I/P, Inc 2012. *Method and apparatus for active heave compensation*. US Patent No. 8265811.
- Robichaux, L.R., and Hatleskog, J.T., Retsco, Inc. 1993. *Semi-active heave compensation system for marine vessels*. US Patent 5209302.
- Southerland, A., 1970. Mechanical systems for ocean engineering. *Naval Engineers Journal*, 82(5), pp.63-74.

Spong, M.W. et al., 2004. *Robot Dynamics and Control*. 2nd Ed. John Wiley & Sons, Inc.:United States.

Korde, U.A., 1988. Active heave compensation on drill-ships in irregular waves. *Ocean Engineering*, 25(7), pp.541-561.

Young, K.D., Utkin, V.I. and Özgür, Ü., 1999. *A Control Engineer's Guide to Sliding Mode Control*. *IEEE Transactions on control systems technology*, 7(3), pp.328-342.

